

Effects of particle-hole fluctuations on the superfluid transition in two-dimensional atomic Fermi gases

Junru Wu,^{1,2,3} Zongpu Wang,^{1,4} Lin Sun,^{3,2} Kaichao Zhang,^{1,2,3} Chuping Li,^{1,2,3}
Yuxuan Wu,^{1,2,3} Pengyi Chen,^{1,2,3} Dingli Yuan,^{1,2,3} and Qijin Chen^{1,2,3,*}

¹Hefei National Research Center for Physical Sciences at the Microscale and School of Physical Sciences,
University of Science and Technology of China, Hefei, Anhui 230026, China

²Shanghai Research Center for Quantum Science and CAS Center for Excellence in Quantum Information and Quantum Physics,
University of Science and Technology of China, Shanghai 201315, China

³Hefei National Laboratory, University of Science and Technology of China, Hefei 230088, China

⁴Department of Physics, University of Hong Kong, Pokfulam Road, Hong Kong

(Dated: October 28, 2025)

Proper treatment of the many-body interactions is of paramount importance in our understanding of strongly correlated systems. Here we investigate the effects of particle-hole fluctuations on the Berezinskii-Kosterlitz-Thouless (BKT) transition in two-dimensional Fermi gases throughout the entire BCS-BEC crossover. We include self-consistently in the self energy treatment the entire particle-hole T matrix, which constitutes a renormalization of the bare interaction that appears in the particle-particle scattering T matrix, leading to a screening of the pairing interaction and hence a dramatic reduction of the pairing gap and the transition temperature. The BKT transition temperature T_{BKT} is determined by the critical phase space density, for which the pair density and pair mass are determined using a pairing fluctuation theory, which accommodates self-consistently the important self-energy feedback in the treatment of finite-momentum pairing fluctuations. The screening strength varies continuously from its maximum in the BCS limit to essentially zero in BEC limit. In the unitary regime, it leads to an interaction-dependent shift of T_{BKT} towards the BEC regime. This shift is crucial in an attempt to explain experimental data quantitatively, which often depends on the interaction strength. Our findings are consistent with available experimental results in the unitary and BEC regimes and with quantum Monte Carlo simulations in the BCS and unitary regimes.

I. INTRODUCTION

Strongly correlated systems constitute the main challenge and are thus at the heart and frontier of condensed matter physics. Due to the low dimensionality, fluctuations in two dimensions (2D) are usually strong, positioning the system in the strongly correlated regime, for which a proper treatment of interaction effects is of paramount importance, in order to understand various experiments and physical phenomena at a quantitative level.

In the absence of long range order as the Mermin-Wagner theorem [1], phase transition in 2D is in general of the Berezinskii [2], Kosterlitz and Thouless (BKT) [3] type. Indeed, superfluid transitions in ultracold atomic Bose gases have been experimentally found to exhibit a strong BKT nature in 2D [4–6]. BKT transitions have been of wide interest since the most important high T_c superconductors are quasi-2D layered materials [7], for which the low dimensionality is favorable for the formation of the wide-spread pseudogap phenomena, which are arguably attributable to strong fluctuations [8, 9]. It is also the model commonly used for describing the superconducting transition in thin films [10, 11]. Recent exciting discoveries of (quasi-)2D superconductors [12–15] have added to the interest in 2D phase transitions. The BKT nature of the superfluid transition in 2D atomic Fermi gases has also been experimentally confirmed [16, 17]. There are also, albeit not many, theoretical studies of the BKT superfluid transition

in a 2D Fermi system for both weak and strong pairing interactions, e.g., Ref. [18, 19].

In this paper, we report our study on the important yet often neglected effect of the particle-hole fluctuations on 2D Fermi gas superfluidity, to which similar studies has not been reported in the literature [19]. Similar to its 3D counterpart, we find that particle-hole fluctuations lead to a screening to the pairing interaction, causing a shift of the superfluid transition curve toward the BEC regime as a function of the pairing strength. This substantially suppresses T_c and the gap in the BCS and unitary regimes, and has an important physical significance when comparing between theory and experiment.

It is important to note that there has been a historical controversy surrounding 2D fermionic superfluids, dating back to Kosterlitz and Thouless [3], which primarily concerns observable signatures and the applicability of BKT physics. It is not straightforward to apply the BKT theory based on the XY model to fermionic superfluids. In the XY model, in which the superfluid density n_s/m provides the phase stiffness, it is the phase fluctuations of the vortex type that dominate the destruction of the quasi-long range superfluid order and drive the system into a disordered normal state. Unlike the superfluids of true bosons, however, the superfluid density is also suppressed by the pair-breaking Bogoliubov quasiparticle excitations as the temperature T increases. In addition, both the density and the mass of the bosons (i.e., fermion pair) now depend on the temperature and the pairing interaction strength, except in the deep BEC regime. Therefore, computing the superfluid density using a mean-field approximation would yield a constant value $n_s/m = n/m$ at $T = 0$ (or $n/4m$ from the boson point of view, with $n_B = n/2$ and $m_B = 2m$), inde-

* Corresponding author: qjc@ustc.edu.cn

pendent of the interaction strength. (Following standard notations, here n , m , n_B , m_B and n_s denote total fermion number density, fermion mass, Cooper pair number density, Cooper pair mass, and superfluid number density, respectively.) At finite T , the pair-breaking effect due to quasiparticle excitations can be partly accounted for via solving the mean-field BCS gap equation, leading to a mean-field result of $(n_s/m)^{\text{BCS}}$. However, not being able to properly take care of the effective pair mass and pair number density is thus expected to give rise to an overestimate of the superfluid transition temperature T_{BKT} . Indeed, the fact T_{BKT} , as measured experimentally in 2D atomic Fermi gases, varies with interaction strength, reflects that both n_B and M_B vary with the interaction.

The pair number density at given temperature and interaction is normally governed by the pair dispersion. The latter, or equivalently pair mass, can, in principle, be extracted from the pair propagator. However, there are not many calculations of the fermionic T_{BKT} in the literature [20–23], partly due to the inapplicability of the simple XY model directly to the Fermi system. The fact that $(n_s/m)^{\text{BCS}}$ decreases with temperature below T_{BKT} in the BCS regime manifests the fact that amplitude fluctuations play an important role. Therefore, the superfluid transition in a 2D Fermi gas has a much richer physics than the simple XY model can capture. To account for the finite temperature and interaction effects, Wu et al [24] and Wang et al Ref. [18] determined T_{BKT} using the critical phase space density criterion, based on a quantum Monte Carlo simulation [25] along with experimental support [17]. A pairing fluctuation theory [26] that was developed to address the pseudogap phenomena in 3D superconductors was used to determine the effective pair number density n_B and pair mass M_B , which reflect the effects of both amplitude and phase fluctuations, governed by temperature and interaction strength. Nevertheless, this earlier work considered only the particle-particle channel of the T -matrix.

It has been known that particle-hole fluctuations may play an important role in the 3D superfluid behavior, despite that they are often neglected in theoretical treatments of superconductivity [27]. Gor'kov and Melik-Barkhudarov (GMB) [28] first found that the lowest order particle-hole fluctuations may reduce both T_c and the zero temperature gap Δ_0 by a factor of 0.44 in a BCS superconductor. The study of the GMB effect at the lowest order were extended to atomic Fermi gases in the continuum [29] or an optical lattice [30]. The effect beyond the lowest order, by including the full particle-hole T -matrix in a ladder approximation has been studied without [31] and with [32] the self-energy feedback.

In 2D, there have been no similar studies in the literature, however. It is the purpose of the present work to investigate the effect of particle-hole fluctuations on the atomic Fermi gas superfluidity in 2D. The low dimensionality further enhances the strong pairing fluctuations, which are already present when the interaction is strong. The very BKT nature of the transition requires that there is already a sizable pairing amplitude, i.e., (pseudo)gap, at T_{BKT} . Therefore, this necessitates the self-consistent inclusion of the self-energy feedback in (both the particle-particle and) the particle-hole T -matrices. Here we incorporate the particle-hole channel contributions

to the pairing fluctuation theory [26, 32, 33], and thus go beyond previous studies [18, 24]. This pairing fluctuation theory includes self-consistently the finite-momentum pairing fluctuations in the single-fermion self energy, and has successfully addressed multiple high T_c [26, 33–35] and atomic Fermi gas experiments [36–39]. In particular, it features naturally a pseudogap in 3D unitary Fermi gases, which has been unequivocally corroborated by a recent experiment [40]. Following the previous work in 3D [32], we show that the particle-hole T -matrix serves as a renormalized pairing interaction, which is to appear in the T -matrix in the usual particle-particle channel. We find that the particle-hole fluctuations lead to a screening to the pairing interaction, and the inverse pairing interaction is effectively shifted by the temperature-dependent, angular-averaged (at two different levels) particle-hole susceptibility $\langle\chi_{\text{ph}}\rangle$, which approaches a negative constant, $-m/2\pi$, in the BCS limit and increases gradually in the crossover regime toward zero in the BEC limit. In result, the particle-hole channel shifts the T_{BKT} curve towards the BEC regime as a function of pairing strength. Furthermore, comparison shows that the inclusion of particle-hole channel leads to a better overall agreement between our calculated T_{BKT} with the results from experiment and quantum Monte Carlo simulations.

II. THEORETICAL FORMALISM

A. Overview of the Pair Fluctuation Theory without the Particle-Hole Channel

To be self-contained, we first recapitulate the pairing fluctuation theory [24, 26, 33] without including the particle-hole channel. This serves as a basis, on top of which the particle-hole channel effect is built. Note that here we will consider only the formalism without the superfluid order parameter, tailored for 2D in the absence of a true long range order.

We consider a 2D Fermi gas with a short-range s -wave attractive interaction $V_{\mathbf{k},\mathbf{k}'} = U < 0$, as described by a generic grand canonical Hamiltonian [33], which includes pairing with a finite momentum \mathbf{q} . The free fermion dispersion is given by $\xi_{\mathbf{k}} = \epsilon_{\mathbf{k}} - \mu \equiv \mathbf{k}^2/2m - \mu$, with chemical potential μ . The Fermi momentum is $\hbar k_F = \sqrt{2\pi n \hbar}$, and Fermi energy $E_F \equiv k_B T_F = \hbar^2 k_F^2/2m$. As usual, we shall use the natural units, and set $\hbar = k_B = 1$ and the volume to unity [26].

The fermions acquire self energy via pair binding and unbinding. Our approximated equations, derived via an equations of motion approach [41, 42], can be cast into a T matrix formalism, with a mix of bare Green's function $G_0(K) = (i\omega_l - \xi_{\mathbf{k}})^{-1}$ and full Green's function $G(K)$ in the pair susceptibility $\chi(Q) = \sum_K G(K)G_0(Q - K)$. Here we use the four-momentum notation, $K \equiv (i\omega_l, \mathbf{k})$ and $Q \equiv (i\Omega_n, \mathbf{q})$, $\sum_K \equiv T \sum_{l,\mathbf{k}}$ and $\sum_Q \equiv T \sum_{n,\mathbf{q}}$, with ω_l and Ω_n being Matsubara frequencies for fermions and bosons, respectively [43]. The T -matrix $t(Q)$ is given by $t(Q) = U/[1 + U\chi(Q)]$,

with the self energy

$$\Sigma(K) = \sum_Q t(Q)G_0(Q - K).$$

The Thouless criterion (for superfluid transition in 3D) requires $t^{-1}(Q = 0) = U^{-1} + \chi(0) = 0$. In order to accommodate the absence of long range order in 2D, we generalize the Thouless criterion to allow for a very small but finite pair chemical potential μ_p , $U^{-1} + \chi(0) = t^{-1}(0) \propto \mu_p$. In this way, $t(Q)$ is highly peaked around $Q = 0$. Thus the main contribution to $\Sigma(K)$ comes from the vicinity of zero momentum for pairs, leading to the approximation of $\Sigma(K) \approx -\Delta^2 G_0(-K)$, where we define the pseudogap as $\Delta^2 = -\sum_Q t(Q)$. With this approximation, the full Green's function takes a simple BCS-like form and is given by

$$G(K) = \frac{u_{\mathbf{k}}^2}{i\omega_n - E_{\mathbf{k}}} + \frac{v_{\mathbf{k}}^2}{i\omega_n + E_{\mathbf{k}}},$$

where $E_{\mathbf{k}} = \sqrt{\xi_{\mathbf{k}}^2 + \Delta^2}$, $u_{\mathbf{k}}^2 = (1 + \xi_{\mathbf{k}}/E_{\mathbf{k}})/2$, and $v_{\mathbf{k}}^2 = (1 - \xi_{\mathbf{k}}/E_{\mathbf{k}})/2$. Then one obtains a generalized BCS-like gap equation,

$$a_0\mu_p = \sum_{\mathbf{k}} \left[\frac{1 - 2f(E_{\mathbf{k}})}{2E_{\mathbf{k}}} - \frac{1}{2\epsilon_{\mathbf{k}} + \epsilon_B} \right], \quad (1)$$

where a_0 is the coefficient of the linear Ω term in the Taylor expansion of the inverse T -matrix. Here the gap equation has been regularized via $U^{-1} = -\sum_{\mathbf{k}} 1/(2\epsilon_{\mathbf{k}} + \epsilon_B)$, where the two-body binding energy $\epsilon_B = 1/ma_{2D}^2$ with the 2D scattering length a_{2D} [44]. The fermion number constraint $n = 2\sum_{\mathbf{k}} G(K)$ yields

$$n = \sum_{\mathbf{k}} \left[1 - \frac{\xi_{\mathbf{k}}}{E_{\mathbf{k}}} + 2\frac{\xi_{\mathbf{k}}}{E_{\mathbf{k}}} f(E_{\mathbf{k}}) \right], \quad (2)$$

where $f(x)$ is the Fermi distribution function.

To extract the pair dispersion, one can Taylor expand t^{-1} near $Q = 0$ and analytically continue to the real frequency axis, with $(i\Omega_l \rightarrow \Omega + i0^+)$, so that

$$t^{-1}(\Omega, \mathbf{q}) \approx a_1\Omega^2 + a_0(\Omega - \Omega_{\mathbf{q}}^0 + \mu_p), \quad (3)$$

where $\Omega_{\mathbf{q}}^0 = \mathbf{q}^2/2M_B$. Consequently, the definition of the pseudogap yields

$$a_0\Delta^2 = \sum_{\mathbf{q}} \left[1 + 4\frac{a_1}{a_0}(\Omega_{\mathbf{q}}^0 - \mu_p) \right]^{-1/2} b(\Omega_{\mathbf{q}}), \quad (4)$$

where $b(x)$ is the Bose distribution function and $\Omega_{\mathbf{q}} = \left[\sqrt{a_0^2 + 4a_0a_1(\Omega_{\mathbf{q}}^0 - \mu_p)} - a_0 \right] / 2a_1$ represents the pair dispersion. The coefficients a_0 , a_1 , M_B are determined via the expansion process. Except in the weak coupling BCS regime, the a_1 term serves as a small quantitative correction and can often be neglected, so that $\Omega_{\mathbf{q}} \approx \Omega_{\mathbf{q}}^0 - \mu_p$.

B. BKT Criterion

At $T = 0$ where $\mu_p = 0$, Eqs. (1) and (2) give $\mu = E_F - \epsilon_B/2$ and $\Delta = \sqrt{2E_F\epsilon_B}$ [45]. At finite temperature, the summation in Eq. (4) analytically leads to $\frac{a_0}{a_1} - \sqrt{\frac{a_0}{a_1}(\frac{a_0}{a_1} - 4\mu_p)} = 2T \ln(1 - e^{-\mathcal{D}_B})$, which reduces to $\mu_p = T \ln(1 - e^{-\mathcal{D}_B})$ in the BEC regime. Here $n_B = a_0\Delta^2$ represents the pair density, and \mathcal{D}_B is the bosonic phase space density. Thus μ_p is primarily determined by \mathcal{D}_B at given temperature, indicating that the BKT transition may occur when \mathcal{D}_B is large enough so that μ_p becomes sufficiently close to zero [17, 18, 24, 46]. Moreover, in the BEC regime, a large \mathcal{D}_B provides a sharp peak distribution of the bosonic number density at zero momentum via $b(-\mu_p) = e^{\mathcal{D}_B} - 1$, signaling a quasi-condensation [24]. Alternatively, when the phase space density becomes large enough, the wave functions of neighboring pairs start to overlap with each other, and hence help to establish quasi-long-range phase coherence.

When approached from the high-temperature region [4, 47], the bosonic BKT transition occurs when $\mathcal{D}_B(T)$ reaches a critical value $\mathcal{D}_B(T_{\text{BKT}})$ [46]. Estimates of $\mathcal{D}_B(T_{\text{BKT}})$ for fermionic superfluids are provided in Refs. [16, 17], with values ranging from approximately 4.9 to 6.45. In comparison, the analogous systems in atomic Bose gases typically hover around 8 [6]. The lowest value, $\mathcal{D}_B(T_{\text{BKT}}) = 4.9$, which is the closest to the factor of 4 in the usual BKT relation, was reported to offer the best fit for the experimental results on Fermi gases [17]. Thus we choose $\mathcal{D}_B(T_{\text{BKT}}) = 4.9$, and the BKT transition temperature T_{BKT} is determined by

$$\frac{n_B}{M_B} = \frac{4.9}{2\pi} T_{\text{BKT}}. \quad (5)$$

C. Contributions of the Particle-Hole Channel

Following Ref. [32], we introduce the contribution of the particle-hole channel, by renormalizing the pairing strength in $t(Q)$, which leads to a new full T -matrix $t_2(Q)$ that includes both particle-particle and particle-hole contributions. The expression for $t_2(Q)$ is given by

$$t_2(Q) = \frac{1}{t_{\text{ph}}^{-1}(K + K' - Q) + \chi(Q)},$$

which self-consistently includes the self-energy feedback, with K, K' being the external fermion momentum. Here the particle-hole channel T -matrix $t_{\text{ph}}^{-1}(Q') = U^{-1} + \chi_{\text{ph}}(Q')$ describes the particle-hole scattering, and the particle-hole susceptibility $\chi_{\text{ph}}(Q') = \sum_K G(K)G_0(K - Q')$, where the particle-hole momentum $Q' = K + K' - Q$. Moreover, assuming that the fermions near the Fermi surface dominate the particle-hole channel contributions, we replace the particle-hole susceptibility with an average $\langle \chi_{\text{ph}} \rangle$ on or near the Fermi surface, where the frequency part of the particle-hole susceptibility is set to 0 with $i\Omega'_n = 0$ [48], leading to a zero imaginary part of $\chi_{\text{ph}}(Q')$ and therefore a purely real $\langle \chi_{\text{ph}} \rangle$ [32].

We have proposed two methods for averaging $\chi_{\text{ph}}(Q')$, referred to as level 1 and level 2, respectively. The level 1 average involves an on-shell and elastic scattering on the Fermi surface, with $|\mathbf{k}| = |\mathbf{k}'| = k_\mu = \sqrt{2m \max(\mu, 0)}$, where the momentum part of $\chi_{\text{ph}}(Q')$ is determined by $|\mathbf{q}'| = |\mathbf{k} + \mathbf{k}'| = k_\mu \sqrt{2(1 + \cos\theta)}$. Here $\chi_{\text{ph}}(Q')$ is averaged over scattering angles θ (between \mathbf{k} and \mathbf{k}'). This averaging process, focusing solely on the Fermi surface, is commonly used in the literature on the studies of induced interactions. In contrast, the level 2 average considers that the states within the energy range $\xi_{\mathbf{k}} \in [-\min(\Delta, \mu), \Delta]$ of a typical s-wave superconductor are most significantly affected by pairing (for $\mu > 0$). Hence, for the level 2 average, while keeping the on-shell and elastic scattering, the average is performed over a range of $|\mathbf{k}|$ such that the quasi-particle energy $E_{\mathbf{k}} \in [\min(E_{\mathbf{k}}), \min(\sqrt{E_{\mathbf{k}}^2 + \Delta^2})]$, where $\min(E_{\mathbf{k}}) = \Delta$ if $\mu > 0$, or $\min(E_{\mathbf{k}}) = \sqrt{\mu^2 + \Delta^2}$ if $\mu < 0$.

Then with this frequency and momentum independent $\langle\chi_{\text{ph}}\rangle$, the new full T -matrix $t_{\text{eff}}(Q)$ reads

$$t_{\text{eff}}(Q) = \frac{1}{U^{-1} + \langle\chi_{\text{ph}}\rangle + \chi(Q)}. \quad (6)$$

The gap equation with the particle-hole channel effect is modified into

$$a_0\mu_{\text{p}} = \langle\chi_{\text{ph}}\rangle + \sum_{\mathbf{k}} \left[\frac{1 - 2f(E_{\mathbf{k}})}{2E_{\mathbf{k}}} - \frac{1}{2\epsilon_{\mathbf{k}} + \epsilon_{\text{B}}} \right], \quad (7)$$

while the other equations remain unchanged.

Equations (2), (4), and (7) form a closed set of self-consistent equations, which can be used to solve for $(\mu, \Delta, \mu_{\text{p}})$, along with T_{BKT} via the BKT criterion given by Eq. (5).

Throughout the BCS-BEC crossover, $\langle\chi_{\text{ph}}\rangle$ remains negative as a function of the coupling strength. From Eq. (7), the particle-hole channel constitutes a renormalization of the pairing interaction, with a net effect given by replacing $1/U$ with $1/U_{\text{eff}} \equiv 1/U + \langle\chi_{\text{ph}}\rangle$. Diagrammatically, this amounts to replacing the bare interaction U with the full particle-hole T -matrix t_{ph} in the particle-particle scattering diagrams [32]. Given the negative sign of $\langle\chi_{\text{ph}}\rangle$, one can see immediately that $|U_{\text{eff}}| < |U|$. Thus U_{eff} represents a weaker, screened pairing interaction.

III. NUMERICAL RESULTS AND DISCUSSIONS

A. Behaviors of the particle-hole susceptibility

First, we present in Fig. 1 the (level 1) angular average of the particle-hole susceptibility at zero frequency as a function of momentum k , under the on-shell condition $|\mathbf{k}| = |\mathbf{k}'| = k$. Here we focus on the unitary case at $T = T_{\text{BKT}}$ (black solid line) and zero-temperature (red dashed line), and $\langle\chi_{\text{ph}}(0, |\mathbf{k} + \mathbf{k}'|)\rangle$ is calculated using the corresponding solution of $(\Delta, \mu, \mu_{\text{p}})$ at $T_{\text{BKT}}/T_{\text{F}} = 0.079$ and $\ln(k_{\text{F}}a_{2\text{D}}) = 0$, solved in the absence of particle-hole fluctuations. The slight

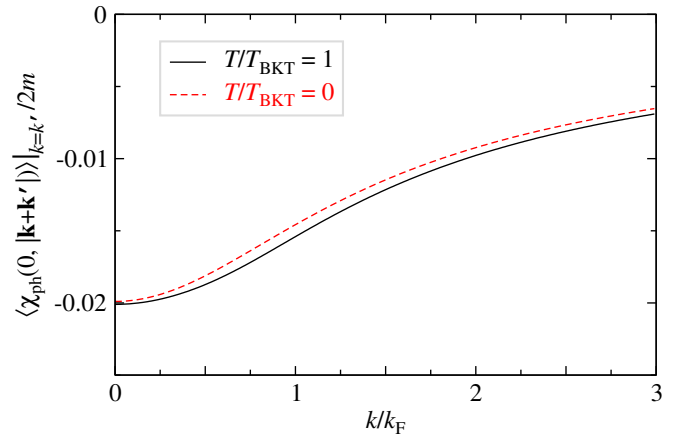


Figure 1. Angular average of the on-shell particle-hole susceptibility $\langle\chi_{\text{ph}}(0, |\mathbf{k} + \mathbf{k}'|)\rangle/2m$ with $k = k'$ as a function of momentum k/k_{F} at unitarity $\ln(k_{\text{F}}a_{2\text{D}}) = 0$ for $T = 0$ and $T = T_{\text{BKT}}$, where $T_{\text{BKT}}/T_{\text{F}} = 0.079$ and the corresponding Δ , μ and μ_{p} are calculated without the particle-hole channel effect.

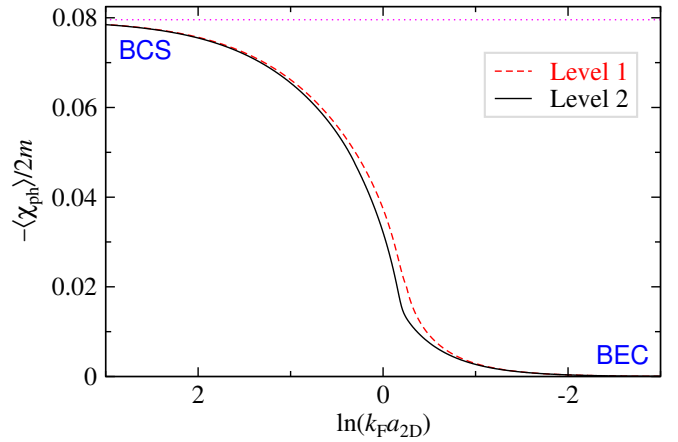


Figure 2. $-\langle\chi_{\text{ph}}\rangle/2m$ at $T = T_{\text{BKT}}$, averaged at both level 1 (red dashed) and level 2 (black solid line), as a function of $\ln(k_{\text{F}}a_{2\text{D}})$ throughout BCS-BEC crossover. The magenta dotted line indicates the BCS limit value, $1/4\pi$, given by $-\langle\chi_{\text{ph}}\rangle = m/2\pi$.

difference between these two curves reveals a weak temperature dependence. Importantly, both curves show a strong momentum dependency, with the amplitude decreasing monotonically as the momentum rises. Note that the momentum dependencies in 2D appear distinct from those in 3D [32], where $\langle\chi_{\text{ph}}(0, |\mathbf{k} + \mathbf{k}'|)\rangle$ exhibits a nonmonotonic momentum dependence at low T for the unitary case.

Shown in Fig. 2 is $-\langle\chi_{\text{ph}}\rangle$ at $T = T_{\text{BKT}}$ as a function of $\ln(k_{\text{F}}a_{2\text{D}})$ throughout the BCS-BEC crossover, averaged at both level 1 (red dashed) and level 2 (black solid curve), along with its BCS limit $1/4\pi \approx 0.0796$, given by $\langle\chi_{\text{ph}}\rangle = -m/2\pi$. The value of $-\langle\chi_{\text{ph}}\rangle/2m$ decreases monotonically with increasing interaction strength and exhibits an exponential behavior in the deep BEC regime for $\ln(k_{\text{F}}a_{2\text{D}}) < -2$. As the gap diminishes, the average at both levels converges in the BCS limit. However, in the crossover regime, the two levels

differ significantly, with a smaller absolute value for the level 2 average. This can be understood from Fig. 1; compared with level 1 averaging, level 2 averaging involves a range of k 's so that the larger k contributions dominates due to its larger phase space area, leading to a smaller absolute value of the average. In other words, level 1 averaging on the Fermi surface only leads to a significant over-estimate of the particle-hole contributions in the unitary regime.

The asymptotic behavior of $\langle\chi_{\text{ph}}\rangle$ can be readily solved analytically in both the BCS and the BEC limits. In the weak coupling limit, where $\ln(k_{\text{F}}a_{2\text{D}}) \rightarrow \infty$, $\Delta \rightarrow 0$, and $T \leq T_{\text{BKT}} \rightarrow 0$, the two levels of average converge to $\chi_{\text{ph}}(Q') \approx \sum_K G_0(K)G_0(K-Q')$. Under the on-shell condition $\xi_{\mathbf{k}} = \xi_{\mathbf{k}-\mathbf{q}'}$, the integrand becomes the derivative of the Fermi function and one readily obtains

$$\chi_{\text{ph}}(0, \mathbf{q}') = \sum_{\mathbf{k}} \frac{f(\xi_{\mathbf{k}}) - f(\xi_{\mathbf{k}-\mathbf{q}'})}{\xi_{\mathbf{k}} - \xi_{\mathbf{k}-\mathbf{q}'}} \approx -\frac{m}{2\pi} = \langle\chi_{\text{ph}}\rangle. \quad (8)$$

We emphasize that this result is independent of the density, due to the constant density of states in 2D. This is to be contrasted with its 3D counterpart, which is proportional to the on-shell momentum k . In the strong coupling limit, where $\ln(k_{\text{F}}a_{2\text{D}}) \rightarrow -\infty$, we have $|\mu| \gg \Delta \gg \epsilon_{\text{F}}$, which indicates that $E_{\mathbf{k}} \approx \xi_{\mathbf{k}} \approx |\mu|$. Thus particle-hole fluctuations are exponentially suppressed, so that $\langle\chi_{\text{ph}}\rangle$ approaches zero.

B. Effect of particle-hole channel on the BKT transition

In this section, we explore the impact of the particle-hole channel on the pairing phenomena and the BKT transition of a 2D Fermi gas. We begin by examining the behavior of the pairing gap Δ at zero temperature with and without the particle-hole channel contributions. Plotted in Fig. 3(a) is Δ as a function of interaction. For comparison, we plot the results both without (black solid line) and with the particle-hole channel effect, with the particle-hole susceptibility $\langle\chi_{\text{ph}}\rangle$ averaged at level 1 (red dashed curve) and level 2 (blue dot-dashed curve), respectively. The corresponding $\langle\chi_{\text{ph}}\rangle$ is shown in Fig. 3(b). For all cases, Δ decreases monotonically from BEC to BCS, as expected. A substantial reduction of Δ by the particle-hole fluctuations occurs in the crossover and BCS regimes. In the BEC regime, $\langle\chi_{\text{ph}}\rangle$ approaches zero, rendering the particle-hole effect negligible. Consistent with Fig. 3(b), level 2 averaging showed a weaker particle-hole effect, and thus a smaller reduction of $\Delta(T=0)$. Note that in Fig. 3(b), there exists a kink around $\mu=0$ in $\langle\chi_{\text{ph}}\rangle$ for both levels of averaging, mainly because the Fermi surface shrinks to zero abruptly with a finite slope as a function of increasing pairing strength. The Fermi function in the integrand of $\langle\chi_{\text{ph}}\rangle$ becomes a step function at zero T , resulting in a delta function in the derivative of the integrand of $\langle\chi_{\text{ph}}\rangle$ and hence a discontinuity when crossing $\mu=0$ (See Appendix A for details). This slope discontinuity becomes more prominent in the level 2 average, since the range for $k < k_{\mu}$ in the average shrinks to zero abruptly when $\mu=0$ [49].

For the effect of the particle-hole channel on the behavior of the BKT transition temperature T_{BKT} , we first analytically es-

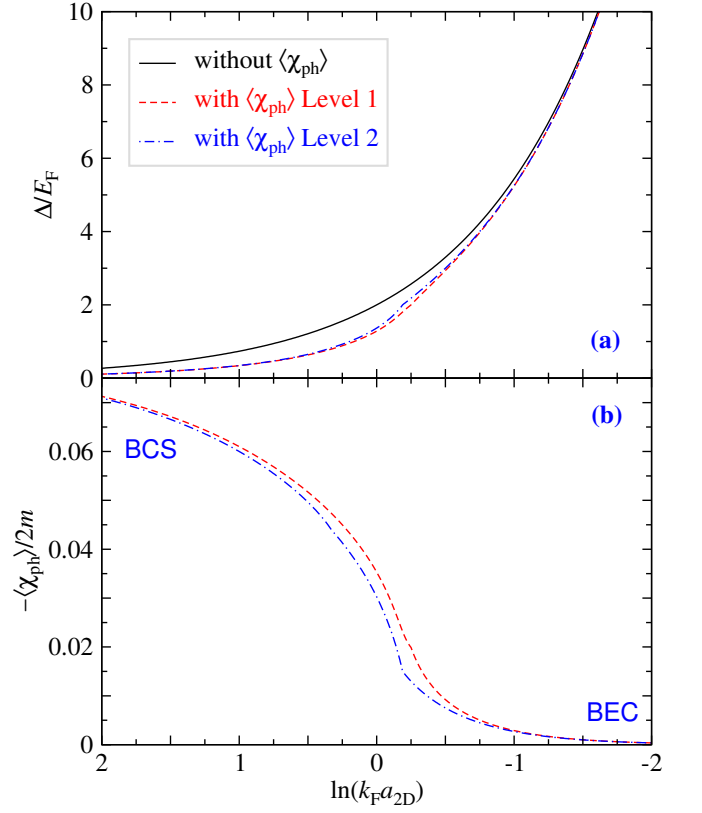


Figure 3. (a) Effect of the particle-hole channel contributions on Δ , along with (b) the corresponding $-\langle\chi_{\text{ph}}\rangle/2m$, at $T=0$, as the function of $\ln(k_{\text{F}}a_{2\text{D}})$ throughout the BCS-BEC crossover. Shown are results without (black solid curve) and with particle-hole channel contributions averaged at level 1 (red dashed) and level 2 (blue dot-dashed curve).

timate the ratio between the two BKT transition temperatures in the BCS limit with and without the particle-hole channel at the same coupling strength, where the latter is denoted as $T_{\text{BKT}}^{\text{BCS}}$. Here $\Delta \rightarrow 0$, so that the following summation can be performed analytically,

$$\sum_{\mathbf{k}} \left[\frac{1 - 2f(\xi_{\mathbf{k}})}{2\xi_{\mathbf{k}}} - \frac{1}{2\epsilon_{\mathbf{k}} + \epsilon_{\text{B}}} \right] = \frac{m}{4\pi} \ln \left(\frac{2e^{2\gamma}\epsilon_{\text{B}}E_{\text{F}}}{\pi^2 T^2} \right),$$

where $\gamma \approx 0.5772157$ is Euler's constant. (A detailed derivation can be found in Appendix B.) Substituting the above relation for the corresponding term in Eqs. (1) and (7), we obtain

$$\frac{T_{\text{BKT}}}{T_{\text{BKT}}^{\text{BCS}}} = e^{2\pi\langle\chi_{\text{ph}}\rangle/m} = e^{-1} \approx 0.37,$$

where we have taken into account that $t^{-1}(0)$ and $t_2^{-1}(0)$ are sufficiently small so that $|t^{-1}(0)|, |t_2^{-1}(0)| \ll |\langle\chi_{\text{ph}}\rangle|$ in the weak coupling limit.

Next, we present in Fig. 4 the effect of the particle-hole channel on the evolution of (a) T_{BKT} , along with (b) Δ , (c) μ , (d) μ_{p} , (e) n_{B} , and (f) M_{B} at T_{BKT} as a function of $\ln(k_{\text{F}}a_{2\text{D}})$. The results without particle-hole fluctuations are presented as the black solid curves. Starting from the weak coupling

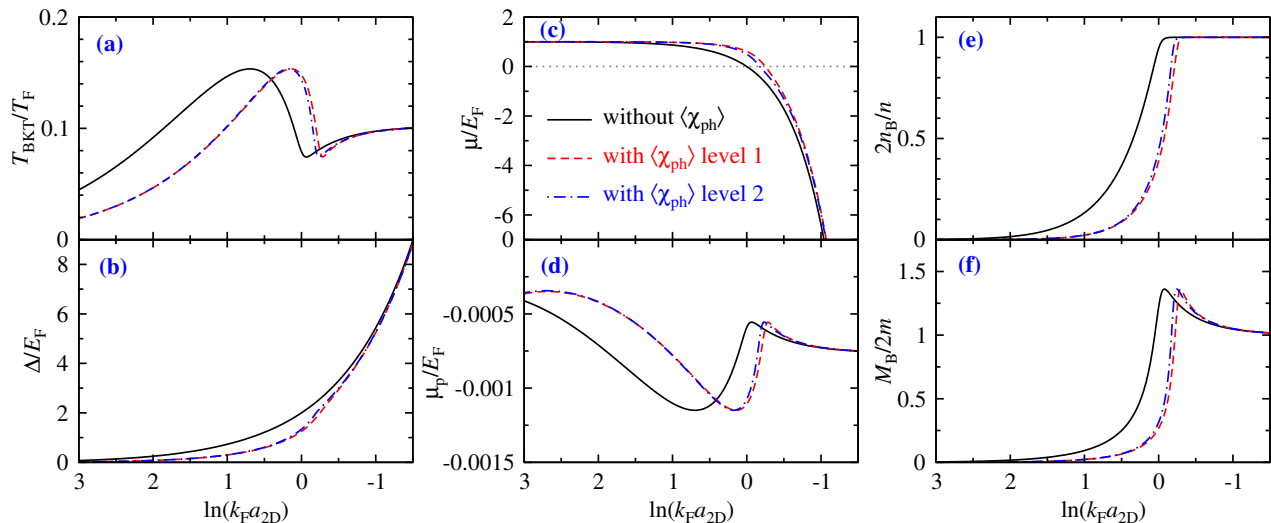


Figure 4. Effect of the particle-hole channel contributions on (a) T_{BKT} , (b) Δ , (c) μ , (d) μ_p , (e) n_B and (f) M_B versus $\ln(k_F a_{2D})$, with the average $\langle \chi_{\text{ph}} \rangle / 2m$ calculated at level 1 (red dashed) and level 2 (blue dot-dashed curves), respectively. They should be compared with the results without the particle-hole effect (black solid curves).

BCS limit (black curve), as the interaction strength increases, T_{BKT} increases, and then reaches a maximum in the intermediate regime, where μ_p reaches a minimum simultaneously. As the interaction strength increases further past the maximum, T_{BKT} decreases and reaches a minimum near unitarity $\ln(k_F a_{2D}) = 0$, where $\mu = 0$. Beyond this point, the system enters the BEC regime, where all fermions pair up with $2n_B/n \approx 1$. The behavior of T_{BKT} is then influenced by the shrinking pair size, as indicated by a decrease in the pair mass M_B toward $2m$, reaching a BEC asymptote $T_{\text{BKT}}/T_F \approx 0.109$. The gap Δ consistently increases with pairing strength. In comparison, the particle-hole channel contributions cause a *non-uniform shift* of all curves toward the BEC regime on the right. This shift is the largest in the BCS limit, and vanishes in the BEC regime, as indicated in Fig. 2. It exhibits a strong dependence on $\ln(k_F a_{2D})$ in the crossover regime. Now the maximum of T_{BKT} occurs closer to unitarity, and the locate for $\mu = 0$ is shifted into the BEC regime. All T_{BKT} curves with and without the particle-hole effect converge to the same BEC asymptote. From Fig. 4(c), we have a tiny $|\mu_p| \leq 1.2 \times 10^{-3} E_F$ throughout the BCS-BEC crossover for all cases. This ensures that $t(Q)$ remains highly peaked at $Q = 0$ and thus validates our pseudogap approximation for the self-energy, $\Sigma(K) \approx -\Delta^2 G_0(-K)$.

Now we investigate in Fig. 5 the evolution of Δ (top row) and μ_p (bottom row) as a function of reduced temperature T/T_{BKT} in the BCS, unitary, and BEC regimes from left to right without (black) and with (red and green) the particle-hole channel effect. The gap Δ remains nearly constant except in the BCS case (f), where a significant decrease can be discerned near T_{BKT} . The value of Δ with the particle-hole channel effect is reduced from the counterpart without the particle-hole channel effect by a factor of $1/e$ in the BCS limit. This reduction factor becomes smaller in the unitary and BEC regimes, consistent with the zero T and T_{BKT} gap behav-

iors as shown in Fig. 3(a) and Fig. 4(b). At the same time, for all cases, μ_p decreases continuously to zero as T decreases, consistent with $\mu_p = 0$ at $T = 0$ for a true long-range-order ground state. Note that below $0.6T_{\text{BKT}}$, μ_p comes essentially zero.

C. Comparison with different results

Finally, in Fig. 6, we compare our theoretical T_{BKT} with available experimental data [16] and QMC results on the BKT transition in 2D Fermi gases, as a function of $\ln(k_F a_{2D})$ throughout the BCS-BEC crossover. Fig. 6(a) presents the measured quasi-condensate fractions N_q/N [16], overlaid on top of which are the theory curves calculated using our pairing fluctuation theory without (black solid) and with (light cyan solid curve) the particle-hole contributions (level 1). The black solid line was previously presented in Ref. [18]. The experimental data are not dense enough to enable a successful detection of the minimum in T_{BKT} near $\ln(k_F a_{2D}) = 0$, nevertheless, it does seem to suggest there is a minimum in the contour of the quasi-condensate fraction. Thus, our theory is consistent with the data, including the presence of the minimum. In Fig. 6(b), we compare our theoretical result of T_{BKT} with a collection of other theories [21–23, 51], and results obtained from Quantum Monte Carlo (QMC) using a 2D lattice model [52]. Also plotted are the experimental results from Refs. [16] and [50]. In the BEC regime, our results both with (black solid) and without (black dashed line) are in quantitative agreement with both experiments. Here the particle-hole susceptibility is averaged at level 1. On the BCS side, the curves of Mulkerin et al [23] and the BCS mean-field treatment are close to our results without particle-hole, suggesting that particle-hole contributions are not included in Mulkerin et al's calculations [23]. Our result with particle-hole contribu-

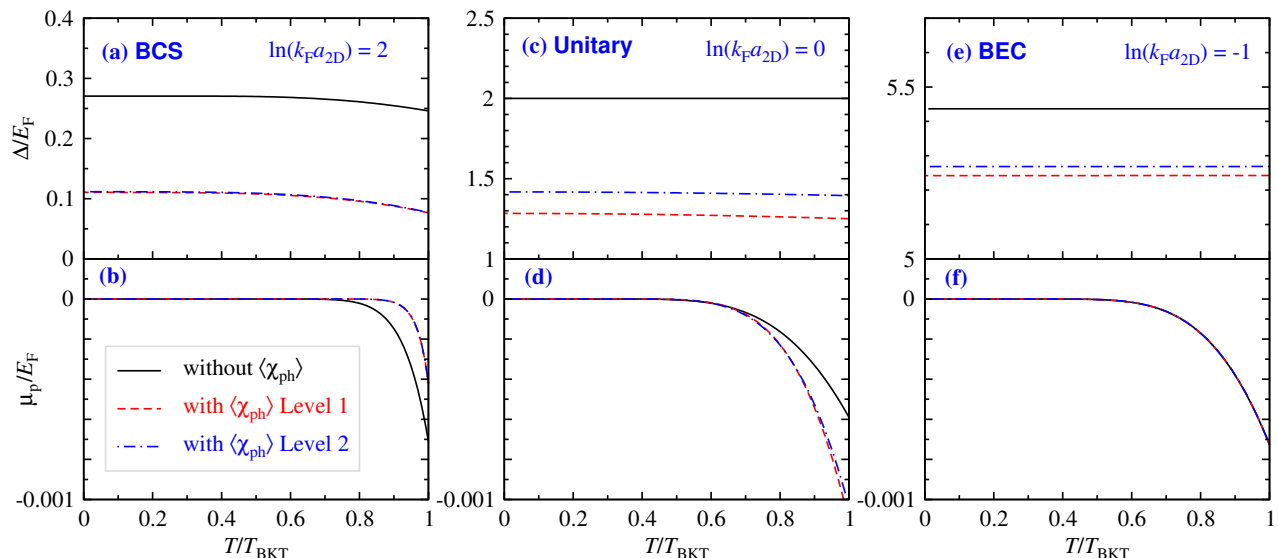


Figure 5. Effect of the particle-hole channel contributions on behaviors of Δ (top row) and μ_p (bottom row), as a function of T/T_{BKT} , with $\ln(k_F a_{2D}) = -1, 0, 2$ from left to right for the BCS, unitary, and BEC regimes, respectively. The black solid curve represents calculations without the particle-hole channel, while the red dashed and green dot-dashed curves include the particle-hole channel effect, using $\langle\chi_{\text{ph}}\rangle/2m$ under level 1 and level 2 averaging, respectively.

tions (black solid) are in good agreement with the QMC result in the infinite L limit, except that QMC does not show a minimum in the unitary regime [52]. The results of Bauer et al [21] and Petrov et al [51] are in good agreement with QMC only in the very weak BCS regime, $\ln(k_F a_{2D}) > 2$. We also notice there is a large difference between the finite ($L = 45$) and infinite lattice QMC results. It is unusual that the result of Bighin et al [22] is far above the BCS mean-field treatment in the BCS limit. It should be noted that the experimental data in the BCS regime are significantly above all theory curves, except the mean-field result. This suggests that some other factors, e.g., nonequilibrium, finite size effect, needs to be considered. Therefore, our result should not be compared with the experimental data in the BCS regime. In short, our results with the particle-hole contributions are consistent with experiment in the unitary and BEC regimes and in good agreement with QMC results in the unitary and BCS regimes. This calls for more data from future experiment.

Note that since the particle-hole susceptibility in Eq. (8) is density independent in 2D, the particle-hole contributions in the weak coupling limit would have already been automatically included, if the 2D scattering length a_{2D} were measured directly through experiment, e.g., by measuring the two-body binding energy in the dilute limit. Instead, a_{2D} is usually calculated from the 3D scattering length as in a deeply confined pancake-shaped trap [53], thus the effect of particle-hole fluctuations should be seriously taken into account when comparing experiment and theory. In Fig. 6, the same definition of a_{2D} was used in both QMC and our present work. This makes it possible to have a good agreement in the BCS regime between QMC and our result with particle-hole fluctuations included. Conversely, one can experimentally determine the particle-hole susceptibility in the BCS limit by measuring the

2D scattering length and comparing with that calculated from a_{3D} , and obtain

$$\langle\chi_{\text{ph}}\rangle = \frac{m}{2\pi} \ln \frac{a_{2D}^{\text{exp}}}{a_{2D}},$$

where a_{2D}^{exp} denotes the experimentally measured 2D scattering length. Nevertheless, away from the weak coupling limit, a nontrivial density dependence should emerge as a nonzero pairing gap develops with increasing pairing strength at a finite density.

IV. CONCLUSIONS

In summary, we have studied the impact of the particle-hole channel on BKT physics in Fermi gases within the context of the BCS-BEC crossover. We introduce the particle-hole channel effect by incorporating an average particle-hole susceptibility, which self-consistently includes the self-energy feedback, leading to an effective renormalization of the pairing strength. The dynamic structure of the angular-averaged particle-hole susceptibility exhibits strong dependencies on momentum and temperature, showing distinct momentum dependencies at low temperatures compared to its 3D counterpart. Furthermore, we perform averaging of the particle-hole susceptibility at two different levels, revealing important physical consequences in the crossover and BCS regimes. The particle-hole channel provides a screening of the pairing interaction and shifts the BKT transition temperature and the pairing gap curves towards the BEC regime as a function of $\ln(k_F a_{2D})$. Additionally, a comparison shows that the BKT transition temperature calculated with the particle-hole channel provides a better fit for the experimental data and QMC re-

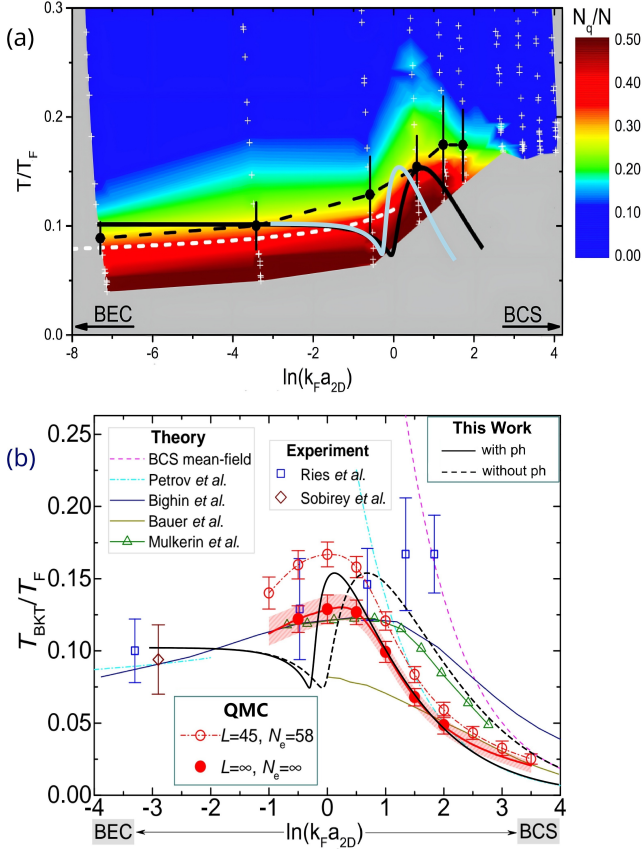


Figure 6. Comparison of theoretical calculations for T_{BKT}/T_F with experiment and QMC results as a function of $\ln(k_F a_{2D})$ throughout the BCS-BEC crossover. (a) Overlay of theoretical T_{BKT} without (black solid line) and with the particle-hole channel calculated with the level 1 average (light cyan solid line), on top of the contour plot of experimentally measured quasi-condensate fractions [16]. Adapted from Ref. [18]. (b) Overlay of our T_{BKT} on top of a collection of experimental data [16, 50] and various theoretical results [21–23, 51, 52]. The black solid and dashed lines represent T_{BKT} calculated using our pairing fluctuation theory with and without the particle-hole contributions, respectively. Here the particle-hole channel effect was calculated with level 1 averaging of $\langle \chi_{\text{ph}} \rangle$. Adapted from Ref. [52].

sults. Future experiments with more elaborate measurements are called for to resolve various discrepancies.

Finally, it should be mentioned that, in addition to the simple averaged particle-hole susceptibility, there are a series of higher order corrections, including a higher order T -matrix [32], which may contribute significant modifications to the present results. In addition, the BKT criterion [18, 24] is merely based on numerical simulations [25] to provide a value of the phase space density. Despite the experimental support [17], an analytical derivation of such a criterion would be highly desirable.

V. ACKNOWLEDGMENTS

This work was supported by the Innovation Program for Quantum Science and Technology (Grant No. 2021ZD0301904).

Appendix A: Slope discontinuity in χ_{ph} across $\mu = 0$ at zero T

The expression for the particle-hole susceptibility $\chi_{\text{ph}}(Q')$ is given by

$$\chi_{\text{ph}}(Q') = \sum_{\mathbf{k}} \left[\frac{f(E_{\mathbf{k}}) - f(\xi_{\mathbf{k}-\mathbf{q}'}) u_{\mathbf{k}}^2}{E_{\mathbf{k}} - \xi_{\mathbf{k}-\mathbf{q}'} - i\Omega'_n} - \frac{1 - f(E_{\mathbf{k}}) - f(\xi_{\mathbf{k}-\mathbf{q}'}) v_{\mathbf{k}}^2}{E_{\mathbf{k}} + \xi_{\mathbf{k}-\mathbf{q}'} + i\Omega'_n} \right].$$

Upon analytical continuation, $i\Omega'_n \rightarrow \Omega' + i0^+$, we separate the retarded $\chi_{\text{ph}}^R(\Omega', \mathbf{q}')$ into real and imaginary parts, $\chi_{\text{ph}}^R(\Omega', \mathbf{q}') = \chi'_{\text{ph}}(\Omega', \mathbf{q}') + i\chi''_{\text{ph}}(\Omega', \mathbf{q}')$. Furthermore, we set $i\Omega'_n = 0$, which leads to $\chi''_{\text{ph}}(0, \mathbf{q}') = 0$, and the real part is expressed as

$$\chi'_{\text{ph}}(0, \mathbf{q}') = \sum_{\mathbf{k}} \left[\frac{f(E_{\mathbf{k}}) - f(\xi_{\mathbf{k}-\mathbf{q}'}) u_{\mathbf{k}}^2}{E_{\mathbf{k}} - \xi_{\mathbf{k}-\mathbf{q}'}} - \frac{1 - f(E_{\mathbf{k}}) - f(\xi_{\mathbf{k}-\mathbf{q}'}) v_{\mathbf{k}}^2}{E_{\mathbf{k}} + \xi_{\mathbf{k}-\mathbf{q}'}} \right].$$

At $T = 0$, we have $f(x) = 1 - \Theta(x)$. Thus $\chi'_{\text{ph}}(0, \mathbf{q}')$ is given by

$$\chi'_{\text{ph}}(0, \mathbf{q}') = \sum_{\mathbf{k}} \left[\frac{\Theta(\xi_{\mathbf{k}-\mathbf{q}'}) - 1}{E_{\mathbf{k}} - \xi_{\mathbf{k}-\mathbf{q}'}} u_{\mathbf{k}}^2 - \frac{\Theta(\xi_{\mathbf{k}-\mathbf{q}'})}{E_{\mathbf{k}} + \xi_{\mathbf{k}-\mathbf{q}'}} v_{\mathbf{k}}^2 \right].$$

Then the derivative of $\chi'_{\text{ph}}(0, \mathbf{q}')$ with respect to μ is given by

$$\begin{aligned} \frac{\partial}{\partial \mu} \chi'_{\text{ph}}(0, \mathbf{q}') &= - \sum_{\mathbf{k}} \left[\frac{1 + \delta(\xi_{\mathbf{k}-\mathbf{q}'})}{E_{\mathbf{k}} + \xi_{\mathbf{k}-\mathbf{q}'}} v_{\mathbf{k}}^2 - \frac{\delta(\xi_{\mathbf{k}-\mathbf{q}'})}{E_{\mathbf{k}} - \xi_{\mathbf{k}-\mathbf{q}'}} u_{\mathbf{k}}^2 \right] \\ &= \begin{cases} - \sum_{\mathbf{k}} \frac{v_{\mathbf{k}}^2}{E_{\mathbf{k}} + \xi_{\mathbf{k}-\mathbf{q}'}} , & \mu < 0, \\ - \sum_{\mathbf{k}} \frac{v_{\mathbf{k}}^2}{E_{\mathbf{k}} + \xi_{\mathbf{k}-\mathbf{q}'}} + \sum_{\phi \in A} \frac{\xi_{\mathbf{k}'}}{E_{\mathbf{k}'}} , & \mu \geq 0, \end{cases} \end{aligned}$$

where $A = \{ \phi : p^2(\cos(\phi)^2 - 1)/2 + \mu \}$ with $\mathbf{k}' = p \cos(\phi) \pm \sqrt{p^2(\cos(\phi)^2 - 1)/2 + \mu}$ given by $\xi_{\mathbf{k}-\mathbf{q}'} = 0$. Thus, an additional term in the derivative of $\chi'_{\text{ph}}(0, \mathbf{q}')$ emerges when the system changes from $\mu < 0$ to $\mu \geq 0$, leading to a slope discontinuity of χ_{ph} .

Appendix B: Analytical result of 2D gap equation in the BCS limit

To obtain an analytical result of the BCS gap equation for the 2D case, we define $\epsilon = \epsilon_{\mathbf{k}}/E_F$, $t = T/T_F$, and $a = \epsilon_B/E_F$.

Since $\mu \approx E_F$, we have

$$\begin{aligned} & \sum_{\mathbf{k}} \left[\frac{1 - 2f(\xi_{\mathbf{k}})}{2\xi_{\mathbf{k}}} - \frac{1}{2\epsilon_{\mathbf{k}} + \epsilon_B} \right] \\ &= \frac{m}{2\pi} \int_0^\infty d\epsilon \left[\frac{\tanh \frac{\epsilon-1}{2t}}{2(\epsilon-1)} - \frac{1}{2\epsilon+a} \right] \\ &= \frac{m}{4\pi} \int_{-\frac{1}{2t}}^\infty dx \left[\frac{\tanh x}{x} - \frac{1}{x + \frac{1}{2t} + \frac{a}{4t}} \right] = \frac{m}{4\pi} \ln \left(\frac{2e^{2\gamma} a}{\pi^2 t^2} \right). \end{aligned}$$

Here we have utilized the fact that $1/2t \gg 1$ to justify the approximation $\tanh(1/2t) = 1$.

-
- [1] N. D. Mermin and H. Wagner, Absence of ferromagnetism or antiferromagnetism in one- or two-dimensional isotropic Heisenberg models, *Phys. Rev. Lett.* **17**, 1133 (1966).
- [2] V. Berezinskii, Destruction of long-range order in one-dimensional and two-dimensional systems possessing a continuous symmetry group. II. Quantum systems, *Sov. Phys. JETP* **34**, 610 (1972).
- [3] J. M. Kosterlitz and D. J. Thouless, Ordering, metastability and phase transitions in two-dimensional systems, *J. Phys. C* **6**, 1181 (1973).
- [4] Z. Hadzibabic, P. Krüger, M. Cheneau, B. Battelier, and J. Dalibard, Berezinskii–Kosterlitz–Thouless crossover in a trapped atomic gas, *Nature* **441**, 1118 (2006).
- [5] P. Cladé, C. Ryu, A. Ramanathan, K. Helmerson, and W. D. Phillips, Observation of a 2D Bose gas: From thermal to quasi-condensate to superfluid, *Phys. Rev. Lett.* **102**, 170401 (2009).
- [6] S. Tung, G. Lamporesi, D. Lobser, L. Xia, and E. A. Cornell, Observation of the presuperfluid regime in a two-dimensional Bose gas, *Phys. Rev. Lett.* **105**, 230408 (2010).
- [7] M. J. Kosterlitz, Kosterlitz-Thouless physics: a review of key issues, *Rep. Prog. Phys.* **79**, 26001 (2016).
- [8] V. M. Loktev, R. M. Quick, and S. G. Sharapov, Phase fluctuations and pseudogap phenomena, *Physics Reports* **349**, 1 (2001).
- [9] Q. J. Chen, Z. Q. Wang, R. Boyack, S. L. Yang, and K. Levin, When superconductivity crosses over: From BCS to BEC, *Rev. Mod. Phys.* **96**, 025002 (2024).
- [10] I. Hetel, T. R. Lemberger, and M. Randeria, Quantum critical behaviour in the superfluid density of strongly underdoped ultrathin copper oxide films, *Nature Physics* **3**, 700 (2007).
- [11] W. Zhao, Q. Wang, M. Liu, W. Zhang, Y. Wang, M. Chen, Y. Guo, K. He, X. Chen, Y. Wang, J. Wang, X. Xie, Q. Niu, L. Wang, X. Ma, J. K. Jain, M. Chan, and Q.-K. Xue, Evidence for berezinskii–kosterlitz–thouless transition in atomically flat two-dimensional pb superconducting films, *Solid State Communications* **165**, 59 (2013).
- [12] I. Božović, X. He, J. Wu, and A. T. Bollinger, Dependence of the critical temperature in overdoped copper oxides on superfluid density, *Nature* **536**, 309 (2016).
- [13] D. F. Agterberg, T. Shishidou, J. O’Halloran, P. M. R. Brydon, and M. Weinert, Resilient nodeless *d*-wave superconductivity in monolayer FeSe, *Phys. Rev. Lett.* **119**, 267001 (2017).
- [14] Y.-T. Hsu, A. Vaezi, M. H. Fischer, and E.-A. Kim, Topological superconductivity in monolayer transition metal dichalcogenides, *Nature Communications* **8**, 14985 (2017).
- [15] Y. Cao, V. Fatemi, S. Fang, K. Watanabe, T. Taniguchi, E. Kaxiras, and P. Jarillo-Herrero, Unconventional superconductivity in magic-angle graphene superlattices, *Nature* **556**, 43 (2018).
- [16] M. G. Ries, A. N. Wenz, G. Zürn, L. Bayha, I. Boettcher, D. Kedar, P. A. Murthy, M. Neidig, T. Lompe, and S. Jochim, Observation of pair condensation in the quasi-2D BEC-BCS crossover, *Phys. Rev. Lett.* **114**, 230401 (2015).
- [17] P. A. Murthy, I. Boettcher, L. Bayha, M. Holzmann, D. Kedar, M. Neidig, M. G. Ries, A. N. Wenz, G. Zürn, and S. Jochim, Observation of the Berezinskii-Kosterlitz-Thouless phase transition in an ultracold Fermi gas, *Phys. Rev. Lett.* **115**, 010401 (2015).
- [18] X. Y. Wang, Q. J. Chen, and K. Levin, Strong pairing in two dimensions: pseudogaps, domes, and other implications, *New Journal of Physics* **22**, 063050 (2020).
- [19] T. Shi, W. Zhang, and C. A. R. S. de Melo, Tighter upper bounds on the critical temperature of two-dimensional superfluids and superconductors from the bcs to the bose regime, *New Journal of Physics* **26**, 093001 (2024).
- [20] S. S. Botelho and C. A. R. S. de Melo, Vortex-antivortex lattice in ultracold fermionic gases, *Physical Review Letters* **96**, 040404 (2006).
- [21] M. Bauer, M. M. Parish, and T. Enss, Universal equation of state and pseudogap in the two-dimensional Fermi gas, *Phys. Rev. Lett.* **112**, 135302 (2014).
- [22] G. Bighin and L. Salasnich, Finite-temperature quantum fluctuations in two-dimensional Fermi superfluids, *Phys. Rev. B* **93**, 014519 (2016).
- [23] B. C. Mulkerin, L. He, P. Dyke, C. J. Vale, X.-J. Liu, and H. Hu, Superfluid density and critical velocity near the Berezinskii-Kosterlitz-Thouless transition in a two-dimensional strongly interacting Fermi gas, *Phys. Rev. A* **96**, 053608 (2017).
- [24] C.-T. Wu, B. M. Anderson, R. Boyack, and K. Levin, Quasi-condensation in two-dimensional Fermi gases, *Phys. Rev. Lett.* **115**, 240401 (2015).
- [25] N. Prokof’ev, O. Ruebenacker, and B. Svistunov, Critical point of a weakly interacting two-dimensional Bose gas, *Phys. Rev. Lett.* **87**, 270402 (2001).
- [26] Q. J. Chen, I. Kosztin, B. Jankó, and K. Levin, Pairing fluctuation theory of superconducting properties in underdoped to overdoped cuprates, *Phys. Rev. Lett.* **81**, 4708 (1998).
- [27] J. R. Schrieffer, *Theory of superconductivity*, 1st ed. (W.A. Benjamin Inc., New York, 1964).
- [28] L. P. Gor’kov and T. K. Melik-Barkhudarov, Contribution to the theory of superconductivity in an imperfect Fermi gas, *Sov. Phys. JETP* **13**, 1018 (1961), [*J. Exptl. Theoret. Phys. (USSR)*]

- 40, 1452-1458 (1961)].
- [29] H. Heiselberg, C. J. Pethick, H. Smith, and L. Viverit, Influence of induced interactions on the superfluid transition in dilute Fermi gases, *Phys. Rev. Lett.* **85**, 2418 (2000).
- [30] D.-H. Kim, P. Törmä, and J.-P. Martikainen, Induced interactions for ultracold Fermi gases in optical lattices, *Phys. Rev. Lett.* **102**, 245301 (2009).
- [31] Z.-Q. Yu, K. Huang, and L. Yin, Induced interaction in a Fermi gas with a BEC-BCS crossover, *Phys. Rev. A* **79**, 053636 (2009).
- [32] Q. J. Chen, Effect of the particle-hole channel on BCS–Bose-Einstein condensation crossover in atomic Fermi gases, *Scientific Reports* **6**, 25772 (2016).
- [33] Q. J. Chen, I. Kosztin, B. Jankó, and K. Levin, Superconducting transitions from the pseudogap state: d-wave symmetry, lattice, and low-dimensional effects, *Phys. Rev. B* **59**, 7083 (1999).
- [34] Q. J. Chen, K. Levin, and I. Kosztin, Superconducting phase coherence in the presence of a pseudogap: Relation to specific heat, tunneling, and vortex core spectroscopies., *Phys. Rev. B* **63**, 184519 (2001).
- [35] Q. J. Chen, J. Stajic, and K. Levin, Applying BCS-BEC crossover theory to high temperature superconductors and ultracold atomic Fermi gases, *Low Temp. Phys.* **32**, 406 (2006), [*Fiz. Nizk. Temp.* **32**, 538-560 (2006)].
- [36] Q. J. Chen, J. Stajic, S. N. Tan, and K. Levin, BCS–BEC crossover: From high temperature superconductors to ultracold superfluids, *Phys. Rep.* **412**, 1 (2005).
- [37] J. Kinast, A. Turlapov, J. E. Thomas, Q. J. Chen, J. Stajic, and K. Levin, Heat capacity of a strongly interacting Fermi gas, *Science* **307**, 1296 (2005).
- [38] Q. J. Chen and K. Levin, Momentum resolved radio frequency spectroscopy in trapped Fermi gases, *Phys. Rev. Lett.* **102**, 190402 (2009).
- [39] Q. J. Chen and J. B. Wang, Pseudogap phenomena in ultracold atomic Fermi gases, *Front. Phys.* **9**, 539 (2014).
- [40] X. Li, S. Wang, X. Luo, Y.-Y. Zhou, K. Xie, H.-C. Shen, Y.-Z. Nie, Q. J. Chen, H. Hu, Y.-A. Chen, X.-C. Yao, and J.-W. Pan, Observation and quantification of the pseudogap in unitary Fermi gases, *Nature* **626**, 288 (2024).
- [41] L. P. Kadanoff and P. C. Martin, Theory of many-particle systems. ii. superconductivity, *Phys. Rev.* **124**, 670 (1961).
- [42] Q. J. Chen, *Generalization of BCS theory to short coherence length superconductors: A BCS-Bose-Einstein crossover scenario*, Ph.D. thesis, University of Chicago (2000), available as arXiv:1801.06266.
- [43] A. L. Fetter and J. D. Walecka, *Quantum theory of many-particle systems* (McGraw-Hill, 1971).
- [44] J. Levinsen and M. M. Parish, Strongly interacting two-dimensional Fermi gases, in *Annual Review of Cold Atoms and Molecules* (World Scientific, 2015) Chap. CHAPTER 1, pp. 1–75.
- [45] M. Randeria, J.-M. Duan, and L.-Y. Shieh, Superconductivity in a two-dimensional Fermi gas: Evolution from Cooper pairing to Bose condensation, *Phys. Rev. B* **41**, 327 (1990).
- [46] N. Prokof'ev and B. Svistunov, Two-dimensional weakly interacting Bose gas in the fluctuation region, *Phys. Rev. A* **66**, 043608 (2002).
- [47] J. M. Kosterlitz and D. J. Thouless, Early work on defect driven phase transitions, *International Journal of Modern Physics B* **30**, 1630018 (2016).
- [48] L. Gor'kov and T. Melik-Barkhudarov, Contribution to the theory of superfluidity in an imperfect Fermi gas, *Sov. Phys. JETP* **13**, 1018 (1961).
- [49] It should be noted that $\mu = 0$ occurs at $\ln(k_F a_{2D}) \approx -0.25$ and -0.175 for level 1 and 2 averaging, respectively, as they are calculated with the self-consistent solutions of T_{BKT} .
- [50] L. Sobirey, N. Luick, M. Bohlen, H. Biss, H. Moritz, and T. Lompe, Observation of superfluidity in a strongly correlated two-dimensional Fermi gas, *Science* **372**, 844 (2021), <https://www.science.org/doi/pdf/10.1126/science.abc8793>.
- [51] D. S. Petrov, M. A. Baranov, and G. V. Shlyapnikov, Superfluid transition in quasi-two-dimensional Fermi gases, *Phys. Rev. A* **67**, 031601 (2003).
- [52] Y.-Y. He, H. Shi, and S. W. Zhang, Precision many-body study of the Berezinskii-Kosterlitz-Thouless transition and temperature-dependent properties in the two-dimensional Fermi gas, *Phys. Rev. Lett.* **129**, 076403 (2022).
- [53] D. S. Petrov and G. V. Shlyapnikov, Interatomic collisions in a tightly confined Bose gas, *Phys. Rev. A* **64**, 012706 (2001).